

RESEARCH

Open Access



# Nucleolin in the cell membrane promotes Ang II-mediated VSMC phenotypic switching by regulating the AT1R internalization function

Nucleolin promotes Ang II-mediated VSMC phenotypic switching

Li Fang<sup>1\*</sup>, Zhijie Shen<sup>1</sup>, Yinzhuang Zhang<sup>1</sup>, Zhuoni Mao<sup>1</sup>, Dan Huang<sup>1</sup> and Chenyu Lou<sup>1</sup>

## Abstract

**Background** Nucleolin (NCL) plays an important regulatory role in angiotensin II (Ang II)-induced phenotypic switching of vascular smooth muscle cells (VSMCs). The aim of this study was to discuss its potential regulatory mechanisms.

**Results** We investigated if the pathways involving Ang II type 1 receptor (AT1R) and PKC/MAPK are responsible for Ang II's effects on VSMC phenotypic switching. Ang II upregulated NCL expression and activated the PKC/MAPK signaling pathway to induce VSMC phenotypic switching. In addition, Ang II promoted the translocation of NCL from the nucleus to the cell membrane. NCL was shown to bind to AT1R, whereas the binding of NCL to AT1R was greatly attenuated after the deletion of the GAR region. In addition, when peptide-N-glycosidase F (PNGase F) was applied, the N-glycosylation of NCL protein and the phenotypic switching of VSMC were inhibited. Ang II-induced AT1R internalization, whereas overexpression of NCL delayed Ang II-induced AT1R internalization by inhibiting AT1R phosphorylation and recruited Rab4 and Rab11 to promote recycling, and knockdown of NCL showed the opposite effect and reversal of AT1R binding by the use of rasarfin reversed the effects of sh-NCL. In vivo experiments, knockdown of NCL expression inhibited Ang II-induced blood pressure rise and vasculopathy.

**Conclusions** Our study demonstrates that NCL promotes Ang II-mediated phenotypic switching of VSMCs by regulating AT1R internalization function.

**Keywords** VSMC phenotypic switching, Ang II, Ang II type 1 receptor, Nucleolin

\*Correspondence:

Li Fang  
fl20083@sina.com

<sup>1</sup>Cardiovascular Department Second Ward, The Affiliated Changsha Hospital of Xiangya School of Medicine, Central South University, Changsha, China



© The Author(s) 2025. **Open Access** This article is licensed under a Creative Commons Attribution-NonCommercial-NoDerivatives 4.0 International License, which permits any non-commercial use, sharing, distribution and reproduction in any medium or format, as long as you give appropriate credit to the original author(s) and the source, provide a link to the Creative Commons licence, and indicate if you modified the licensed material. You do not have permission under this licence to share adapted material derived from this article or parts of it. The images or other third party material in this article are included in the article's Creative Commons licence, unless indicated otherwise in a credit line to the material. If material is not included in the article's Creative Commons licence and your intended use is not permitted by statutory regulation or exceeds the permitted use, you will need to obtain permission directly from the copyright holder. To view a copy of this licence, visit <http://creativecommons.org/licenses/by-nc-nd/4.0/>.

## Introduction

Vascular smooth muscle cells (VSMCs) are the most abundant cells in blood vessels. Vascular injury stimulates the transformation of contractile VSMCs into a dedifferentiated type, also known as synthetic VSMCs, with high migration and proliferation capacity for repairing vascular injury [1]. This process, called phenotypic switching, is often the first step in vascular pathology. VSMC phenotypic switching plays an important role in vascular remodeling and many cardiovascular diseases, including vascular aging, atherosclerosis [2], and aortic aneurysms [3]. Synthetic VSMCs are characterized by increased proliferation and migration, and increased secretion of extracellular matrix (ECM), MMP, pro-inflammatory cytokines, and exosomes [4]. Therefore, inhibition of VSMC phenotypic switching is important for the treatment of cardiovascular diseases.

Under normal physiological conditions, fewer VSMC have a synthetic phenotype, but they can be converted from a contractile to a synthetic phenotype in response to vascular injury or other extracellular stimuli such as angiotensin II (Ang II) [5]. The function of Ang II is mainly dependent on the activation of the G protein-coupled receptor (GPCR) family member Ang II type 1 receptor (AT1R) [6, 7]. Ang II binds to its receptor AT1R at the cell membrane surface and on the one hand activates downstream signaling pathways to exert its biological roles, including AT1R/phospholipase C (PLC)/protein kinase C (PKC), mitogen-activated protein kinases (MAPK), and Janus kinase (JAK)/signal transducer of activation (STAT) signaling pathways; on the other hand, it rapidly undergoes internalization in the form of lattice protein-encapsulated vesicles [8]. The activation of AT1R by Ang II triggers the phosphorylation of the GPCR kinase, promotes binding to  $\beta$ -arrestins, and leads to desensitization, internalization, and altered signaling of GPCR [9, 10]. Due to the classical effects of Ang II, AT1R internalization has been reported to be closely associated with many cardiovascular diseases [11].

Nucleolin (NCL) is a multilocalized protein that is mainly localized to the nucleolus but has also been found to be localized to the cell membrane, cytoplasm, and nucleoplasm [12]. It has been found to alter the distribution of NCL under several stress conditions. Binding to other molecular partners of NCL located on the surface of the plasma membrane regulates cell differentiation, leukocyte trafficking, angiogenesis, and tumorigenesis [13]. Our previous studies revealed that NCL promotes Ang II-induced VSMC phenotypic switching and stimulates up-regulation of AT1R expression, and its role may be related to its cellular shuttling function as well as cell membrane localization [14, 15]. However, the specific relationship between the role of NCL and AT1R needs to be further investigated.

In the present study, we sought to investigate whether NCL could be involved in Ang II-mediated regulation of VSMC phenotypic switching as a novel AT1R-associated protein, and the molecular mechanism of NCL involvement in AT1R signaling.

## Methods

### Cell isolation and treatment

VSMCs were isolated from the de-endothelialized thoracic aorta of mice by applying enzymatic digestion according to a previous report [16, 17]. The de-endothelialized thoracic aorta was isolated from four-week-old male C57BL/6 mice on ice. The aorta was cleaned and rinsed with PBS using a syringe, followed by enzymatic digestion at 37 °C with agitation. After mincing the tissue, a second digestion was performed, and the suspension was filtered through a cell strainer. The cells were then centrifuged and cultured in M199 medium (PM150610, Pricella) with 10% fetal bovine serum (FBS), penicillin/streptomycin, and plasmocin.

To test the effect of Ang II on VSMCs, we constructed the following two groups: Control (VSMCs without any treatment), and Ang II (VSMCs were treated with Ang II for 48 h ( $10^{-5}$  mmol/L, HY-13948, MCE)) [14].

To investigate whether the AT1R and PKC/MAPK pathways mediate the effects of Ang II on VSMC, we constructed the following six groups: Control, Ang II, Ang II + Valsartan (VSMCs were pre-treated with 1  $\mu$ M valsartan (AT1R inhibitor, HY-18204, MCE) for 1 h, and then treated with Ang II) [23], Ang II + LY317615 (VSMCs were pre-treated with 10  $\mu$ M LY317615 (PKC inhibitor, HY-10342, MCE) for 1 h, and then treated with Ang II), Ang II + SP600125 (VSMCs were pre-treated with 10  $\mu$ M SP600125 (JNK inhibitor, HY-12041, MCE) for 1 h, and then treated with Ang II for 48 h), and Ang II + SB203580 (VSMCs were pre-treated with 10  $\mu$ M SB203580 (p38 MAPK inhibitor, HY-10256, MCE) for 1 h, and then treated with Ang II) [18].

To explore the role of glycosylation on NCL, we constructed the following two groups: Ang II and Ang II + peptide-N-glycosidase F (PNGase F).

To test the mechanism of action of NCL on AT1R, we constructed the following four groups: Control, Ang II, Ang II + oe-NC, and Ang II + oe-NCL (VSMCs were treated with Ang II and then transfected with oe-NC (negative control) or oe-NCL (overexpressed-NCL)).

To investigate the mechanism by which NCL mediated the role of Ang II in the VSMC phenotypic switching, we constructed the following four groups: Ang II + sh-NC, and Ang II + sh-NCL (VSMCs were transfected with sh-NC (negative control) or sh-NCL (silenced-NCL) and then treated with Ang II), Ang II + sh-NCL + DMSO (VSMCs were transfected with sh-NCL and then treated with Ang II and DMSO (AWC0148, Abiowell)), Ang

II + sh-NCL + Rasarfin (VSMCs were transfected with sh-NCL and then treated with Ang II and rasarfin (AT1R internalization blocker, 50  $\mu$ M, HY-139950, MCE) for 30 min) [19].

Plasmids construction and transfection

The sequence of oe-NCL (HG-MO010880) was cloned to the pcDNA3.1(+) vector. The sequences of sh-NC (5'-TA CCTGGTACGGTAAACCGTG-3') and sh-NCL (5'-CCT TTCCTACAGTGCAACAAA-3'; HG-LV010880sh1168) were cloned to the pCDH-CMV-MCS-3xFlag-EF1-GFP+ Puro vector with EF-1 $\alpha$  promoter. In addition, to probe the binding of NCL to AT1R, we purchased the NCL $\Delta$ GAR (HG-MO010880-M1) and NCL $\Delta$ GAR $\Delta$ RBD (HG-MO010880-M2) plasmids. The above plasmids were synthesized by HonorGene.

For transfection, 5  $\mu$ L of plasmid solution (concentration: 200 nM) and 5  $\mu$ L of Lipofectamine 2000 (11668500, Thermo Fisher Scientific) were each mixed with 95  $\mu$ L of serum-free DMEM/F12 medium in separate tubes. These mixtures were gently agitated and incubated at room temperature for 5 min. Subsequently, the contents of both tubes were carefully combined to achieve a total volume of approximately 200  $\mu$ L. The combined solution was further incubated at room temperature for an additional 20 min before being evenly dispensed into VSMCs. After a 6-h incubation period at 37  $^{\circ}$ C within the incubator, the cells were replenished with fresh complete culture medium.

Immunofluorescence (IF)

VSMCs were centrifuged for 3 min, the cell substrate was aspirated, and 3  $\mu$ L was pipetted onto a slide, then added 0.3% Trilatone at 37 $^{\circ}$ C for 30 min. The slide was blocked with 5% BSA for 60 min. The sections were incubated with primary antibodies overnight at 4 $^{\circ}$ C, followed by incubation with Goat anti-Rabbit IgG (H + L) Secondary Antibody (AWS0005a, 1:500, Abiowell) at 37  $^{\circ}$ C for 60 min.

The mouse thoracic aorta tissue slices were subjected to dewaxing using xylene and then rehydrated through a series of ethanol concentrations. Following this, the tissue slices were immersed in a 0.01 M citrate buffer with a pH of 6.0, heated to boiling, then the heating was stopped, and the sections were boiled continuously for 20 min, cooled, and washed with PBS. The slices were placed in sodium borohydride solution and treated using 0.3% H<sub>2</sub>O<sub>2</sub> for 15 min. Subsequently, a blocking step and an antibody incubation step are carried out as described above. Moreover, the slices were subjected to a 5-min incubation at 37  $^{\circ}$ C with TYP-570 fluorescent dye. For nuclear visualization, DAPI staining was utilized. The primary antibodies include OPN (ab63856, Abcam),  $\alpha$ -SMA (14395-1-AP, Proteintech), and Ki67 (ab16667, Abcam).

Real-time quantitative PCR (RT-qPCR)

Total RNA was extracted through Trizol and then converted to cDNA by HiFiScript cDNA Synthesis Kit (CW2569, CWBIO). Gene expression was assessed on the ABI 7900 system using Ultra SYBR Mixture (CW2601, CWBIO).  *$\beta$ -actin* was used as an internal reference to calculate via the 2<sup>- $\Delta\Delta$ Ct</sup> method Table 1.

Western blot (WB)

Total protein was extracted from cells by RIPA (AWB0136, Abiowell). After quantification using a BCA kit (AWB0104, Abiowell), total protein was separated by SDS-PAGE and adsorbed on nitrocellulose membranes by gel electrophoresis. Primary antibody include NCL (ab136649, Abcam), AT1R (25343-1-AP, Proteintech), p38 (AWA00938, Abiowell), p-p38 (AWA48964, Abiowell), p-JNK (AWA45692, Abiowell), JNK (AWA45693, Abiowell), p-ERK (AWA01140, Abiowell), ERK (AWA01141, Abiowell), p-PKC $\alpha$  (AWA43973, Abiowell), PKC $\alpha$  (AWA43970, Abiowell),  $\alpha$ -SMA (AWA00778, Abiowell), SM22 $\alpha$  (AWA47343, Abiowell), OPN (AWA43353, Abiowell),  $\beta$ -arrestin1 (#47698, CST),  $\beta$ -arrestin2 (#3857, CST), Clathrin (AWA43132, Abiowell), AP-2 (AWA41820, Abiowell), Caveolae-1 (AWA47438, Abiowell), Rab4 (AWA00556, Abiowell), Rab11 (AWA46835, Abiowell),  $\beta$ -actin (AWA80002, Abiowell), and PCNA (AWA00425, Abiowell) were incubated at 4  $^{\circ}$ C overnight. The HRP-conjugated secondary antibody was incubated.  $\beta$ -actin, and PCNA were used as an internal reference. The original bands were displayed in the supplementary file.

Cell counting kit-8 (CCK-8)

To evaluate cell viability, we conducted the CCK-8 assay (AWC0114a, Abiowell). Each experimental group comprised three replicate wells. Post-seeding, the cells were exposed to 10  $\mu$ L of CCK-8 reagent per well and allowed to incubate for a duration of 4 h. This CCK-8 reagent has the ability to generate a colored formazan compound within viable cells. Subsequently, the absorbance was quantified at a wavelength of 450 nm using an enzyme marker instrument (MB-530, HuiSong).

5-ethynyl-2-deoxyuridine (EDU) staining

The EDU assay kit (C10310, RiboBio) was used to assess cell proliferation. In brief, cells after different treatments were seeded in 96-well plates at a density of 5  $\times$  10<sup>4</sup> cells

Table 1 Primer sequences

Gene	Sequences (5'-3')
M- <i><math>\beta</math>-actin</i>	Forward: 5'- ACATCCGTAAAGACCTCTATGCC - 3' Reverse: 5'- TACTCCTGCTTGCTGATCCAC - 3'
M-NCL	Forward: 5'- GAGGGCGATATCGAGGGTTC - 3' Reverse: 5'- TATCCGCTCTCAGCTCCTCC - 3'

per well. Diluted EDU was then added to each well and incubated overnight. Each well was sequentially incubated with 4% paraformaldehyde for 30 min, 2 mg/mL glycine for 5 min, and 0.5% TritonX-100 for 10 min. Subsequently, 1 × Apollo staining solution was added and incubated for 30 min. After washing with 0.5% TritonX-100, Hoechst33342 reaction solution was added and incubated for 30 min in the dark, followed by re-staining of the nuclei with DAPI. Finally, positive labeling was determined by fluorescence microscopy (CX41-72C02, Olympus) and counted.

#### Scratching assay

Even horizontal lines were drawn on the back of a 6-well plate using a marker pen, and they were marked using a ruler. Next, approximately  $5 \times 10^5$  cells were seeded into each well. Once the cells had evenly spread across the plate, a perpendicular scratch was carefully made using the tip of a pipette. Images of the scratch were captured at 0 h, 24 h, and 48 h.

#### Enzymatic deglycosylation analysis of glycoprotein

In VSMCs treated with AngII, the N-linked oligosaccharides were removed by treating with PNGase F (P0704S, NEB) at 37 °C for 1 h prior to immunoblotting analysis [20]. Specifically, 20 µg of lysed protein was added to 10 µL of 1 × glycoprotein denaturation buffer (containing 0.5% SDS and 40mM DTT) and denatured at 100 °C for 10 min. After the addition of 1% NP-40 and 1 × GlycoBuffer 2, a two-fold diluted PNGase F was introduced, and the reaction mixture was incubated at 37 °C for 1 h. The separation of the reaction products was visualized through SDS-PAGE.

#### Detection of AT1R phosphorylation

As described in previous reports [21], we examined the phosphorylation of AT1R. Briefly, VSMCs were transfected with HA-AT1R (101659, Addgene) and cultured in serum-free medium overnight and then in phosphate-free medium supplemented with [ $^{32}$ P] orthophosphate (342483, Sigma). Cells were lysed and proteins were pulled onto protein A-agarose (11719408001, Roche) using 12CA5 anti-HA antibody (11583816001, Roche). SDS-PAGE separation was then performed as described above. Lane intensity was measured in the ImageJ software and the densitometric quantification of phosphorylation bands normalized to total phosphorylated protein.

#### Co-immunoprecipitation (Co-IP)

To detect the interaction of NCL with AT1R, proteins were isolated from cell lysates using cell lysis buffer (AWB0144, Abiowell), and then incubated with normal

mouse IgG (B900620, Proteintech) or NCL antibody at 4 °C overnight. To achieve protein specificity, the protein complexes were incubated with protein A/G agarose beads for 2 h at 4 °C. Subsequently, the immunocomplexes underwent heat treatment at 95 °C for 5 min before being analyzed using WB. The primary antibodies included NCL and AT1R for WB.

To detect the interaction of AT1R with Rab4, and Rab11, proteins were incubated with normal rabbit IgG (B900610, Proteintech) or AT1R antibody (25343-1-AP, Proteintech). The remaining steps are consistent with the above. The primary antibodies included AT1R, Rab4, and Rab11 for WB.

#### Animal and treatment

Male C57BL/6J mice (4 weeks old, from the Hunan Slake Jinda Laboratory Animal Center) were utilized in the study. After one week of acclimatization, the mice were treated as follows. Mice were anesthetized by intraperitoneal injection of 50 mg/kg sodium pentobarbital, and an osmotic micropump filled with Ang II was implanted subcutaneously. The osmotic pump delivered Ang II at a rate of 400 ng/kg/min per day for 28 d [22]. The Sham group substituted saline for Ang II 7 d before implantation of the Ang II pumps, and the mice received tail-vein injections of the lentiviruses ( $1 \times 10^{11}$  vector genomes) carrying sh-NC and sh-NCL [23]. Blood pressure was detected by the tail-cuff system and five stabilized blood pressures were recorded. After mice were euthanized by intraperitoneal injection of sodium pentobarbital, the thoracic aorta was isolated for subsequent testing.

#### H&E staining

Tissues were collected and fixed using 4% paraformaldehyde. The collected tissues were fixed and subsequently embedded in paraffin. Following this, tissue sections were prepared and stained using a combination of hematoxylin (AWI0001a, Abiowell) and eosin (AWI0029a, Abiowell) stains. The stained sections were covered with a layer of neutral gum and subsequently examined using a light microscope (BA210T, Motic) for further observation.

#### Statistical analysis

All collected data were analyzed using GraphPad Prism 9 software. The results are depicted as mean values with corresponding standard deviations. To assess statistical significance between the two groups, the Student's *t*-test was used. Statistical analyses for comparisons among multiple groups were performed using one-way ANOVA or two-way ANOVA, followed by Tukey's post hoc test. A *p*-value less than 0.05 was considered statistically significant.



## Results

### Ang II stimulates NCL expression and activates PKC/MAPK to induce VSMC phenotypic switching

We demonstrated successful extraction of VSMCs by observing the morphology of our VSMCs isolated from mouse thoracic aorta and the IF results of  $\alpha$ -SMA, a specific VSMC contractile protein (Fig. 1A and B). RT-qPCR and WB results showed increased expression of NCL in VSMCs after treatment with Ang II (Fig. 1C). In addition, Ang II increased the expression of AT1R and promoted the phosphorylation of p38 MAPK, JNK, ERK, and PKC $\alpha$  (Fig. 1D). To investigate whether the AT1R and PKC/MAPK pathways mediate the role of Ang II on VSMC phenotypic switching, we treated VSMCs with valsartan (AT1R inhibitor), LY317615 (PKC inhibitor), SP600125 (JNK inhibitor), and SB203580 (p38 MAPK inhibitor) respectively. We detected contractile phenotypic markers ( $\alpha$ -SMA and SM22 $\alpha$ ) and synthetic phenotypic markers (OPN) in VSMCs. The results demonstrated that, when compared to the Control group, Ang II treatment significantly reduced the expression of  $\alpha$ -SMA and SM22 $\alpha$  while elevating the expression of OPN. Conversely, valsartan, LY317615, and SP600125 treatments significantly reversed the changes induced by Ang II, as shown in Fig. 1E–G. This suggests Ang II promoted the phenotypic switching of VSMCs, and inhibition of the AT1R and PKC/MAPK pathways contributed to the conversion of VSMCs from a synthetic phenotype to a contractile phenotype. Overall, Ang II stimulates NCL expression and activates PKC/MAPK to induce VSMC phenotypic switching.

### Ang II promotes VSMC phenotype switching through NCL

To investigate whether NCL mediates the promotion of Ang II on VSMC phenotypic switching, we silenced NCL expression in VSMCs. RT-qPCR and WB experiments verified that NCL expression was successfully silenced (Fig. 2A). As shown in Fig. 2B and C, Ang II promoted the expression of NCL, and the expression of NCL was suppressed after silencing NCL. In addition, we detected that Ang II promoted the cell viability, proliferation, migration, and phenotypic switching of VSMCs, whereas silencing of NCL partially reversed the effects of Ang II (Fig. 2D–H). These results suggest that Ang II promotes VSMC phenotypic switching through NCL.

### Ang II stimulates NCL translocation to the cell membrane surface to bind to AT1R

We further explored the mechanism of action of NCL involved in the VSMC phenotypic switching. We initially examined the distribution of NCL in VSMCs. Under normal conditions, NCL was predominantly localized in the

nucleus, as depicted in Fig. 3A. Intriguingly, upon stimulation with Ang II, there was a notable increase in NCL expression in the cell membrane and cytoplasm, accompanied by a significant decrease in nuclear localization, as illustrated in Fig. 3B. NCL consists of a number of functional structural domains, including an amino-terminal charged region, a central region consisting of four RNA-binding (RBD) structural domains, and a carboxy-terminal glycine/arginine (GAR)-rich domain [24]. To verify the binding of NCL to AT1R and to further identify the binding site of NCL to AT1R, we deleted the GAR and RBD fragments of NCL (Fig. 3C). Co-IP results showed that WT-NCL bound to AT1R, whereas the binding of NCL $\Delta$ GAR to AT1R was markedly attenuated, and the binding of NCL $\Delta$ GAR $\Delta$ RBD to AT1R was absent (Fig. 3D). These results suggest that Ang II stimulates NCL translocation to the cell membrane surface to bind to AT1R.

### NCL translocation to the cell membrane is regulated by glycosylation

It has been shown that glycosylation is necessary for NCL expression on the cell membrane surface [25]. Therefore, we used PNGase F to test whether NCL translocation is regulated by glycosylation. The WB results demonstrated that when Ang II-induced VSMCs were treated with PNGase F, the reduction of the molecular weight of NCL by about 25–30 kDa was observed (Fig. 4A). In addition, as shown in Fig. 4B, PNGase F reversed the promotional effect of Ang II on the VSMC phenotypic switching. These results suggest that NCL translocation to the cell membrane is regulated by glycosylation.

### NCL delays Ang II-induced AT1R internalization and recruits Rab4 and Rab11 to promote recycling by inhibiting AT1R phosphorylation

By overexpressing NCL in VSMCs, we further explored the mechanism of action of NCL with AT1R. As shown in Fig. 5A, after transfection with oe-NCL, the expression of NCL in VSMCs increased by 266.1% and 166.6% at the mRNA and protein levels, respectively. WB assay revealed that AT1R was mainly expressed at the cell membrane in the Control group, and Ang II activated AT1R and induced AT1R translocation to the cytoplasm, whereas oe-NCL partially reversed the effect of Ang II (Fig. 5B). The detection of endocytosis process-related indicators ( $\beta$ -arrestin2, Clathrin, AP-2, and Caveolae-1) on cell surface receptors indicated that Ang II promoted AT1R internalization, while oe-NCL inhibited this process (Fig. 5C). Since inhibition of GPCR phosphorylation reduces the affinity of the receptor for  $\beta$ -arrestin thereby delaying GPCR

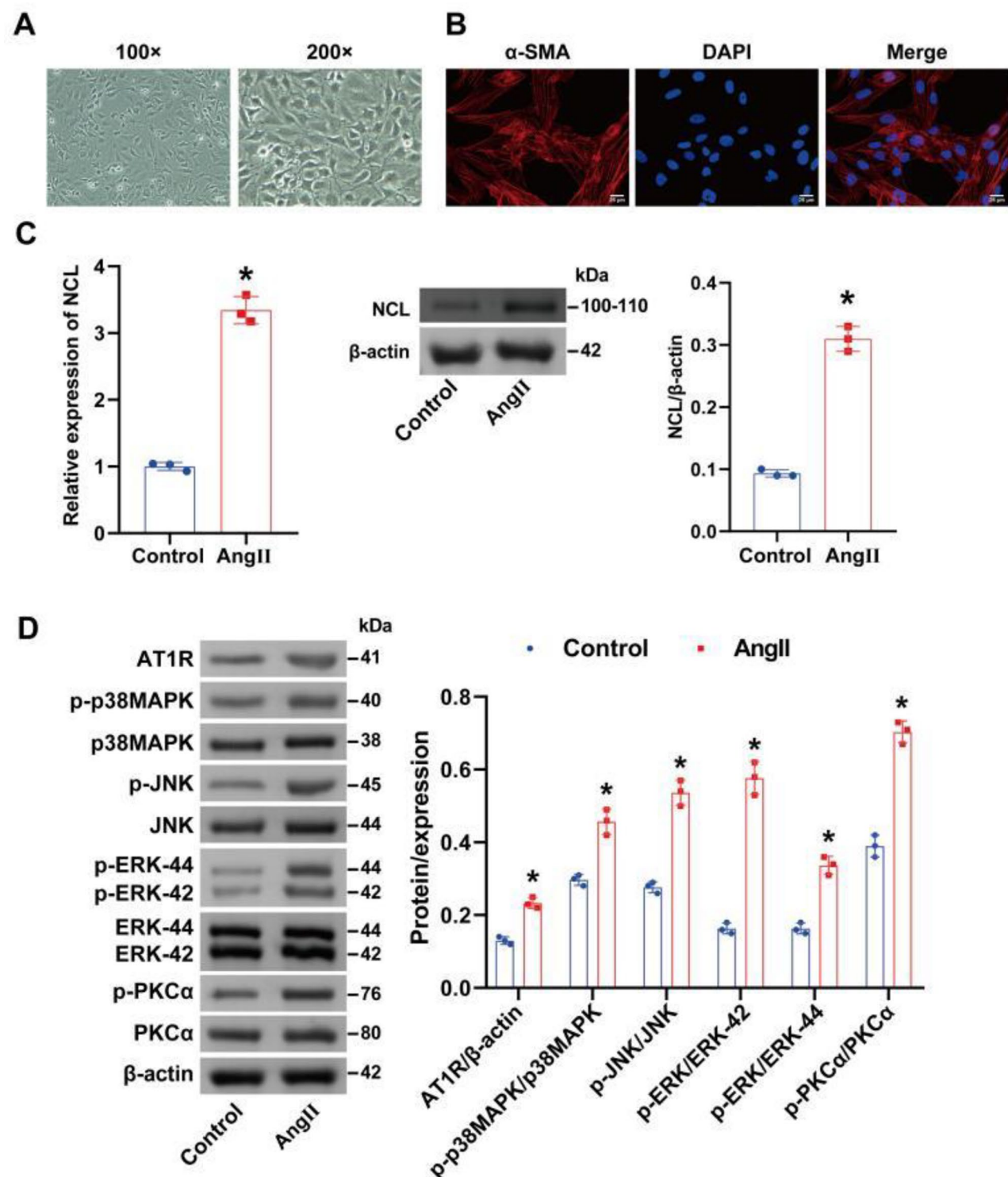


**Fig. 1** Ang II stimulates NCL expression and activates PKC/MAPK to induce VSMC phenotype switching. **A.** Morphology of isolated VSMCs. Scale bar = 100 μm. **B.** IF assay for detecting α-SMA expression. Scale bar = 25 μm. **C.** RT-qPCR and WB analysis of NCL expression in VSMCs without and with Ang II treatment. **D.** WB analysis of AT1R, p-p38MAPK/p38MAPK, p-JNK/JNK, p-ERK/ERK, and p-PKCα/PKCα expression in VSMCs without and with Ang II treatment. \**p* < 0.05 vs. Control. **E.** WB analysis of α-SMA, SM22α, and OPN expression in VSMCs. **F-G.** IF assay for detecting α-SMA and OPN expression in VSMCs. VSMCs were treated with Ang II and valsartan, LY317615, SP600125 or SB203580, respectively. Scale bar = 25 μm. \**p* < 0.05 vs. Control, #*p* < 0.05 vs. Ang II. *n* = 3

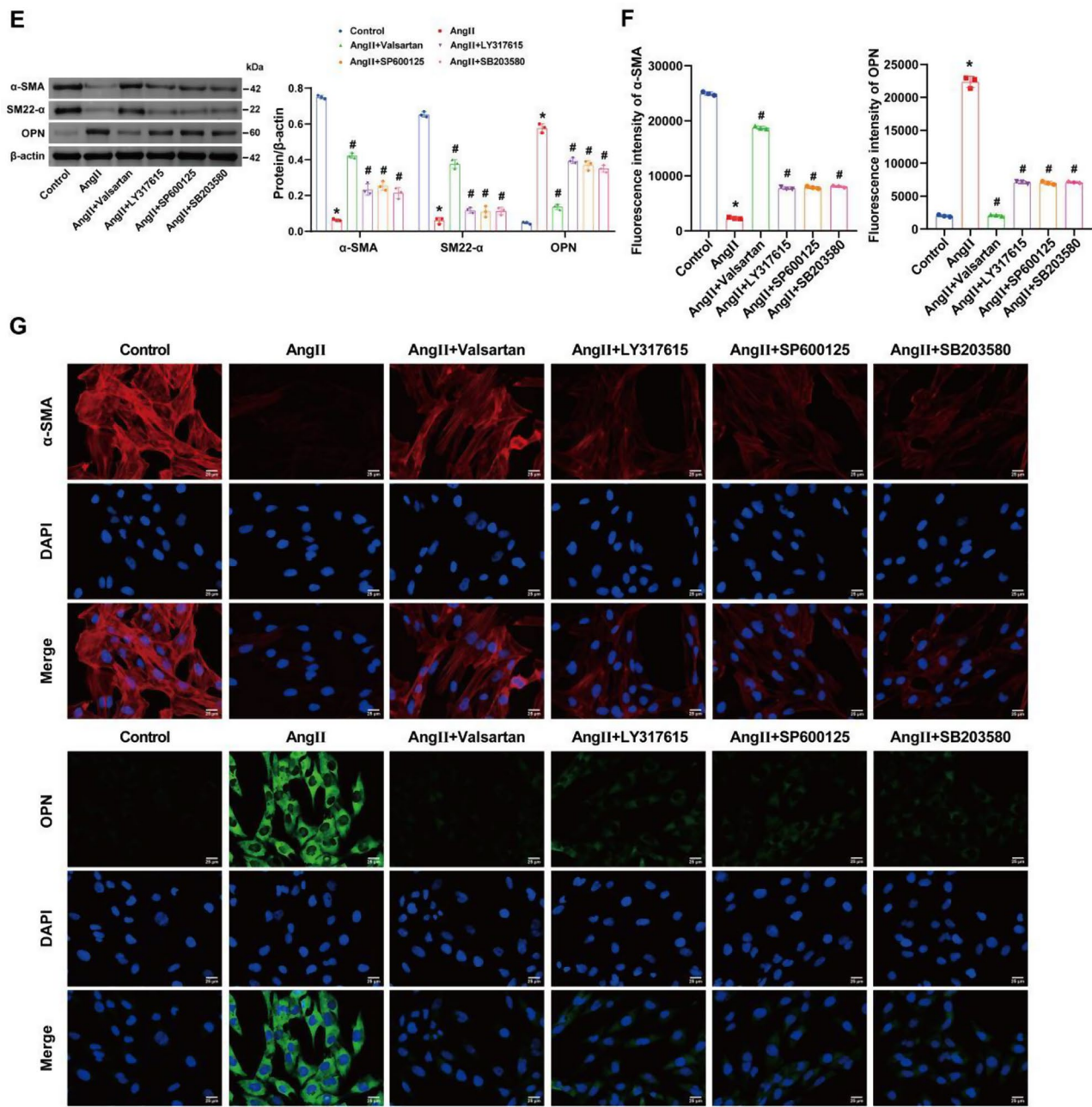


**Fig. 1** (continued)

internalization [26]. Therefore, we also examined the effect of NCL on AT1R phosphorylation. The results showed that Ang II promoted AT1R phosphorylation, while oe-NCL reversed this effect (Fig. 5D). Recirculation of AT1R is coordinately regulated by Rab4 and Rab11 [27]. We re-validated the AT1R's interaction with Rab4 and Rab11 by Co-IP experiments, which showed that AT1R interacted with Rab4 and Rab11,

respectively (Fig. 5E). In addition, we also examined the effect of NCL on Rab4 and Rab11. WB results showed that Ang II increased the expression of Rab4 and Rab11, while oe-NCL further increased their expression (Fig. 5F). These results suggest that NCL delays Ang II-induced AT1R internalization and recruits Rab4 and Rab11 to promote recycling by inhibiting AT1R phosphorylation.



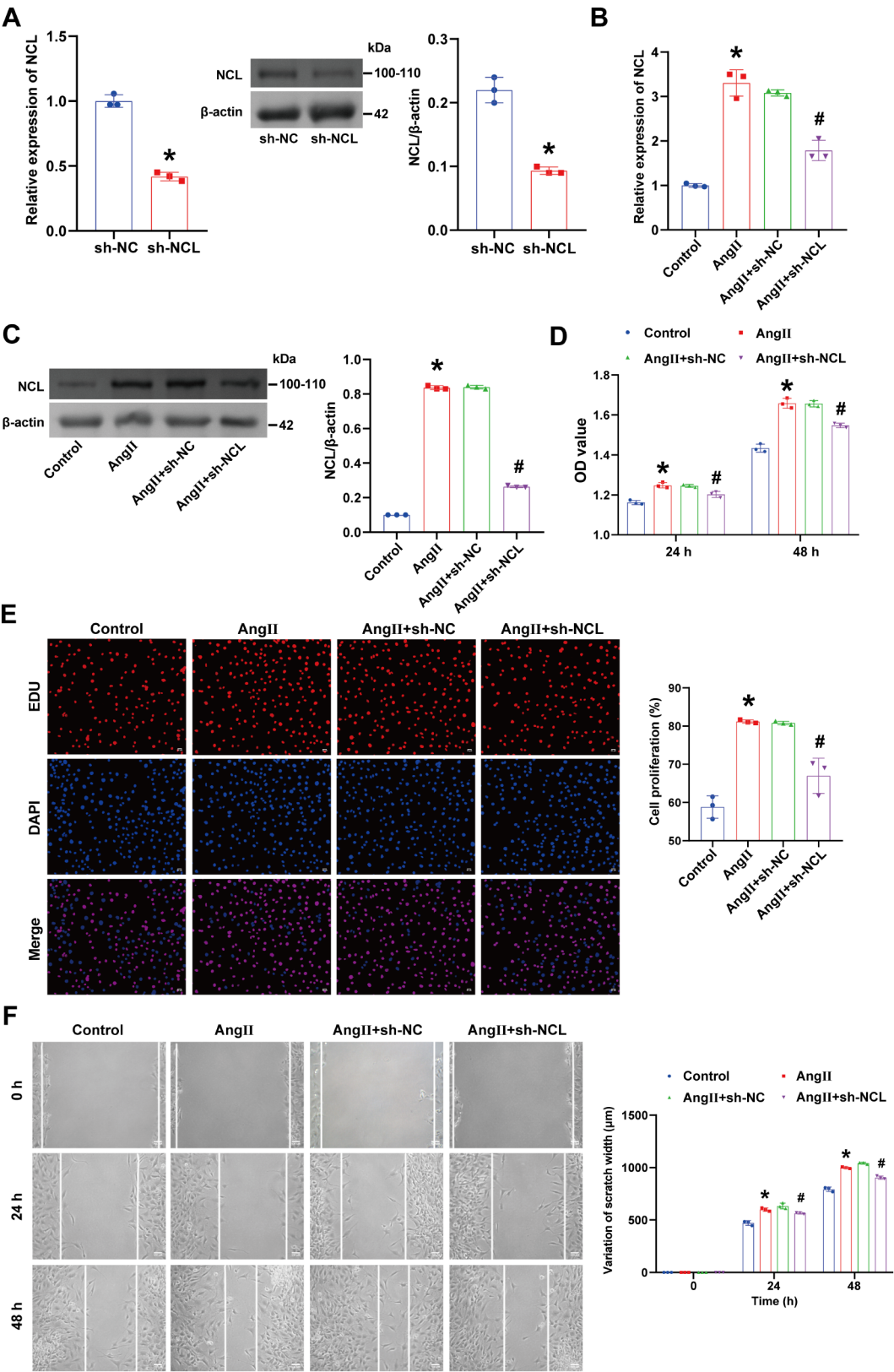


**Fig. 2** (See legend on next page.)



(See figure on previous page.)

**Fig. 2** Ang II promotes VSMC phenotypic switching through NCL. **A.** RT-qPCR and WB analysis of NCL expression in VSMCs transfected with sh-NC or sh-NCL. \* $p < 0.05$  vs. sh-NC. **B–C.** RT-qPCR and WB analysis of NCL expression in VSMCs. **D.** CCK-8 assay for evaluating cell viability of VSMCs. **E.** EDU assay for detecting cell proliferation in VSMCs. Scale bar = 50  $\mu$ M. **F.** Scratch assay for detecting cell migration in VSMCs. Scale bar = 100  $\mu$ M. **G.** WB analysis of  $\alpha$ -SMA, SM22 $\alpha$ , and OPN expression. **H.** IF assay for detecting  $\alpha$ -SMA and OPN expression in VSMCs. Scale bar = 25  $\mu$ M. VSMCs were transfected with sh-NC or sh-NCL and then treated with Ang II. \* $p < 0.05$  vs. Control, # $p < 0.05$  vs. Ang II + sh-NC.  $n = 3$

### NCL induces VSMC phenotypic switching by reducing Ang II-induced AT1R internalization resulting in sustained AT1R activation

To investigate whether the effect of NCL on AT1R internalization is critical in mediating VSMC phenotypic switching, we applied the AT1R internalization blocker rasarfin. sh-NCL was shown to promote AT1R internalization while rasarfin inhibited the process by detecting indicators related to the endocytosis process and AT1R phosphorylation (Fig. 6A and B). Meanwhile, sh-NCL reduced the expression of Rab4 and Rab11, suggesting that sh-NCL inhibited AT1R recirculation, while rasarfin reversed this effect (Fig. 6C). In addition, as shown in Fig. 6D–G, rasarfin reversed the inhibitory effect of sh-NCL on the proliferation, migration, and phenotypic switching of VSMCs. These results suggest that NCL induces VSMC phenotypic switching by reducing Ang II-induced AT1R internalization leading to sustained AT1R activation.

### NCL promotes VSMC phenotypic switching in mice

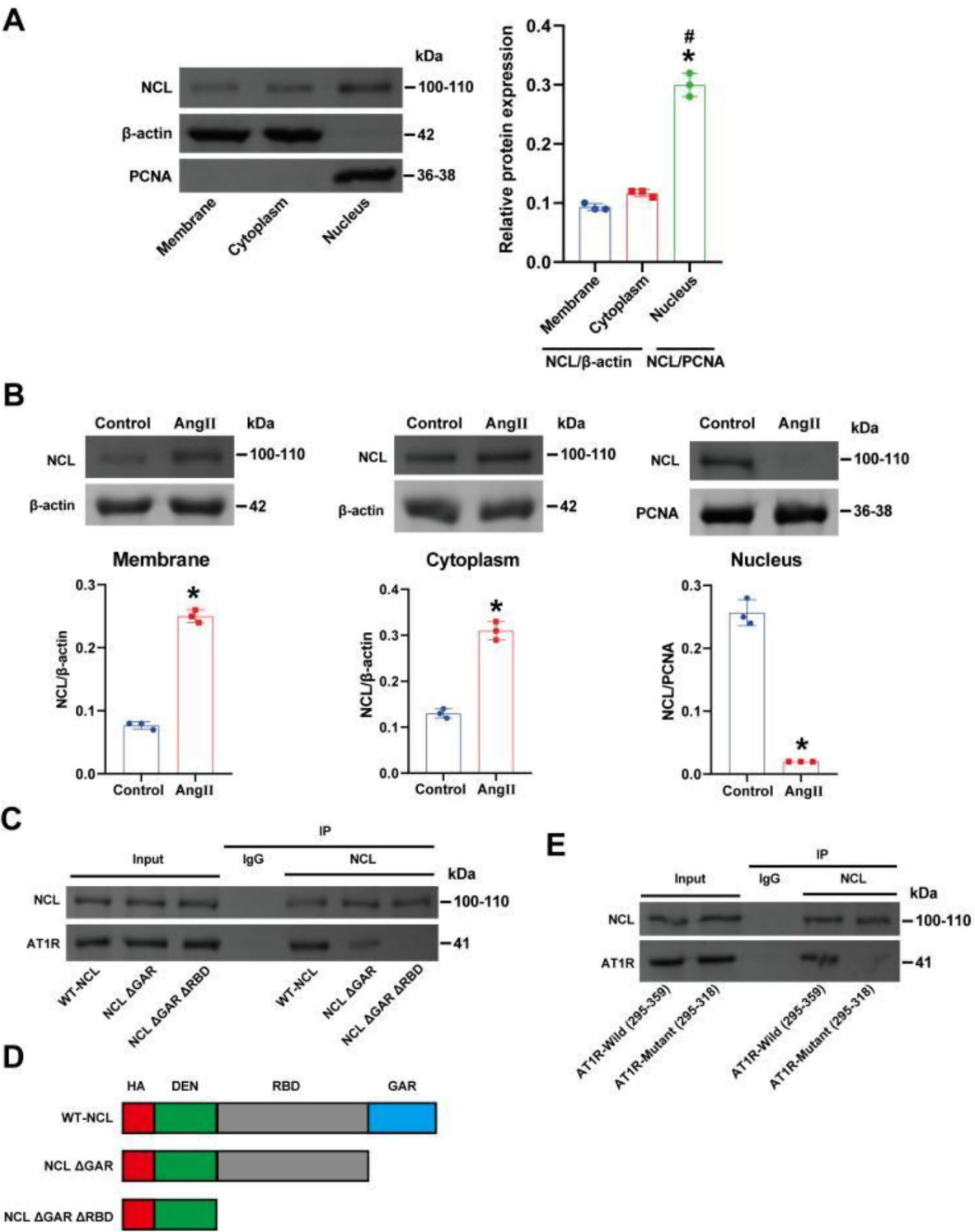
To further validate the effect of NCL on VSMC phenotypic transition in vivo, we constructed a mouse model knocking down the expression of NCL using Ang II treatment and injection of sh-NC or sh-NCL lentiviruses via tail vein. RT-qPCR and WB results revealed a significant decrease in the expression of NCL in mice in the sh-NCL group, showing reductions of 78.23% and 53.75% at the mRNA and protein levels, respectively, compared to the sh-NC group (Fig. 7A). These findings indicate a successful knockdown of NCL expression in mice. By examining the blood pressure of mice in each group over 28 days, it was found that Ang II significantly elevated the blood pressure of mice, and sh-NCL reversed this effect (Fig. 7B). In addition, H&E staining of isolated mouse thoracic aortas showed that the intimal layer of the thoracic aorta in the Sham group consisted of a layer of endothelial cells on top of an internal elastic lamina, the Ang II group and the Ang II + sh-NCL group exhibited increased medial aortic thickness and perivascular fibrosis as well as aortic tissues that showed significant adhesions, dilatation,

and entrapment, and sh-NCL attenuated these phenomena (Fig. 7C). Further, the WB result showed that the expression of NCL was increased in the thoracic aorta of mice in the Ang II group as compared with the Sham group, whereas the expression of NCL was decreased by the application of sh-NCL (Fig. 7D). IF results showed that Ang II promoted Ki67 expression, which was reversed by sh-NCL (Fig. 7E). As shown in Fig. 7F–H, Ang II promoted AT1R endocytosis and recycling and facilitated VSMC phenotypic switching, whereas sh-NCL further enhanced the promotion of AT1R endocytosis by Ang II, while reversing the promotion of AT1R recycling and VSMC phenotypic switching by Ang II. In addition, the expression of the PKC/MAPK pathway was also examined, and the results showed that Ang II activated the PKC/MAPK pathway, while sh-NCL inhibited the PKC/MAPK pathway (Fig. 7I). These results suggest that NCL promotes VSMC phenotypic switching in mice.

### Discussion

In this study, we identified NCL as a novel AT1R-associated protein and elucidated the molecular mechanism by which NCL is involved in the Ang II-induced VSMC phenotypic switching. Ang II stimulates AT1R activation at the plasma membrane of VSMCs and up-regulates the intracellular NCL, which localizes to the plasma membrane through its shuttling property and binds to AT1R, inhibits AT1R internalization by regulating AT1R phosphorylation and recycling, and affects PKC/MAPK downstream signaling pathways, leading to the sustained activation of AT1R signaling and inducing VSMC phenotypic switching. The upregulated NCL, through its shuttling properties, localized to the plasma membrane and bound to AT1R, inhibited AT1R internalization by regulating AT1R phosphorylation and recycling, and affected the PKC/MAPK downstream signaling pathway, leading to the sustained activation of AT1R signaling and VSMC phenotypic switching.

Five AT1R-associated proteins have been identified, such as Ang II type 1 receptor-associated protein (ATRAP), Ang receptor-associated protein 1 (ARAP1),



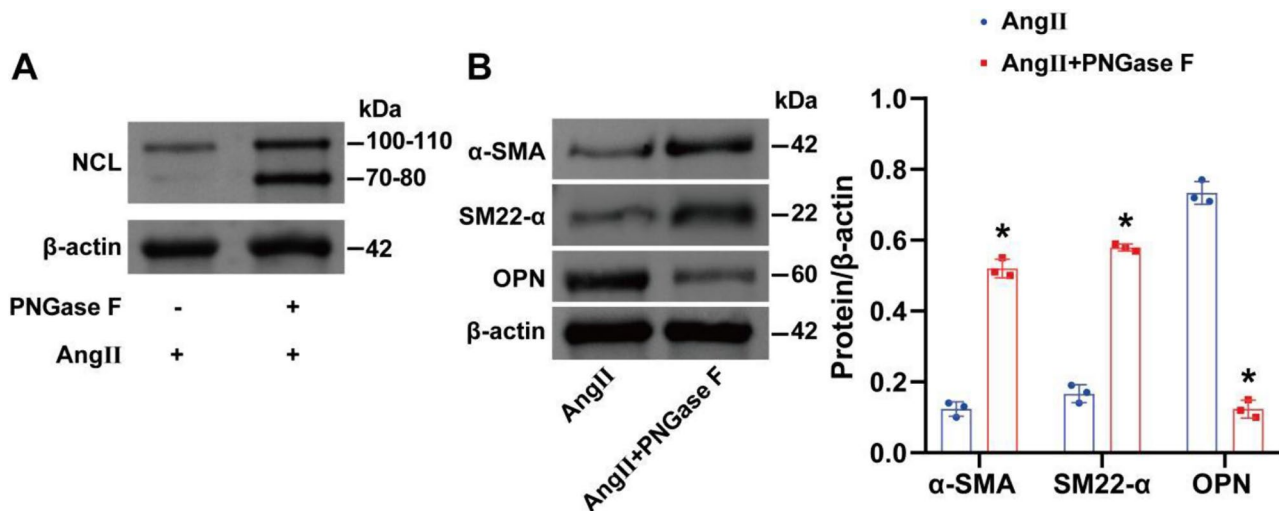


**Fig. 4** NCL translocation to the cell membrane is regulated by glycosylation. **A.** WB analysis of the glycosylation changes in NCL protein extracted from VSMCs was treated with Ang II and PNGase F. **B.** WB analysis of α-SMA, SM22α, and OPN expression in VSMCs. VSMCs were treated with Ang II and PNGase F. \* $p < 0.05$  vs. Ang II.  $n = 3$

GABAA receptor-associated protein (GABARAP), metalloendopeptidase 24.15 (EP24.15), and GDP/GTP-converting factor-like protein (GLP), which are all specifically bind to the carboxyl terminus of AT1R protein and mediate AT1R internalization [8]. Little is known about other AT1R-associated proteins on the cell membrane surface of VSMCs that are involved in regulating VSMC phenotypic switching. Consistent with our previous studies [14, 15], Ang II stimulation of VSMCs resulted in up-regulation of NCL expression and translocation of NCL from the nucleus to the cytoplasm and cell membrane. In addition, the promotional effect of Ang II on phenotypic switching was abolished after the down-regulation of NCL expression. These results confirm that NCL up-regulation plays an important regulatory role in Ang II-induced VSMC phenotypic switching, and that this role may depend on its cytosolic localization. Ang II function is mainly mediated by its receptor, AT1R. Ang II binds to AT1R on the surface of the cell membrane and activates the downstream signaling pathway, PKC/MAPK, to exert its biological roles [28]. Therefore, we speculated that NCL might act as a novel AT1R-related protein involved in Ang II-induced VSMC phenotypic switching by regulating the function of AT1R. This conjecture was confirmed by our results. Co-IP results showed that NCL bound to AT1R, and the binding of NCL to AT1R was significantly attenuated when the GAR structural domain of NCL was knocked down. The GAR structural domain is the decisive factor contributing to the localization of NCL at the plasma membrane

[29]. This further suggests that NCL binds to AT1R at the cell membrane. In addition, NCL undergoes complex N- and O-glycosylation in extra-nuclear isoforms, and N-glycosylation is required for its expression at the cell membrane [30]. We inhibited the N-glycosylation of NCL proteins by applying PNGase F, which significantly inhibited the phenotypic switching of VSMCs. This also provides a new basis for the application of glycosylation inhibitors in regulating VSMC phenotypic switching. However, in the present study, we were unable to directly observe the intracellular localization of NCL via IF and failed to directly measure changes in the glycosylation level of NCL, which represent limitations of this research. We plan to address this shortcoming in future research endeavors.

A decrease in the cell membrane surface density of the AT1R along with an increase in intracellular AT1R levels is thought to be an increase in receptor internalization, and enhanced receptor internalization reduces the likelihood of receptor and agonist reorganization at the plasma membrane, thereby decreasing the receptor's sensitivity to agonists [31]. In recent years, internalization of AT1R has played an important role in maintaining cardiovascular homeostasis, and a decrease in AT1R internalization is closely associated with cardiovascular diseases (e.g., hypertension) caused by abnormal AT1R activation [32]. However, the mechanisms that reduce AT1R internalization are not fully understood. The process of AT1R internalization consists of four components (binding of the agonist Ang II to the receptor AT1R, receptor

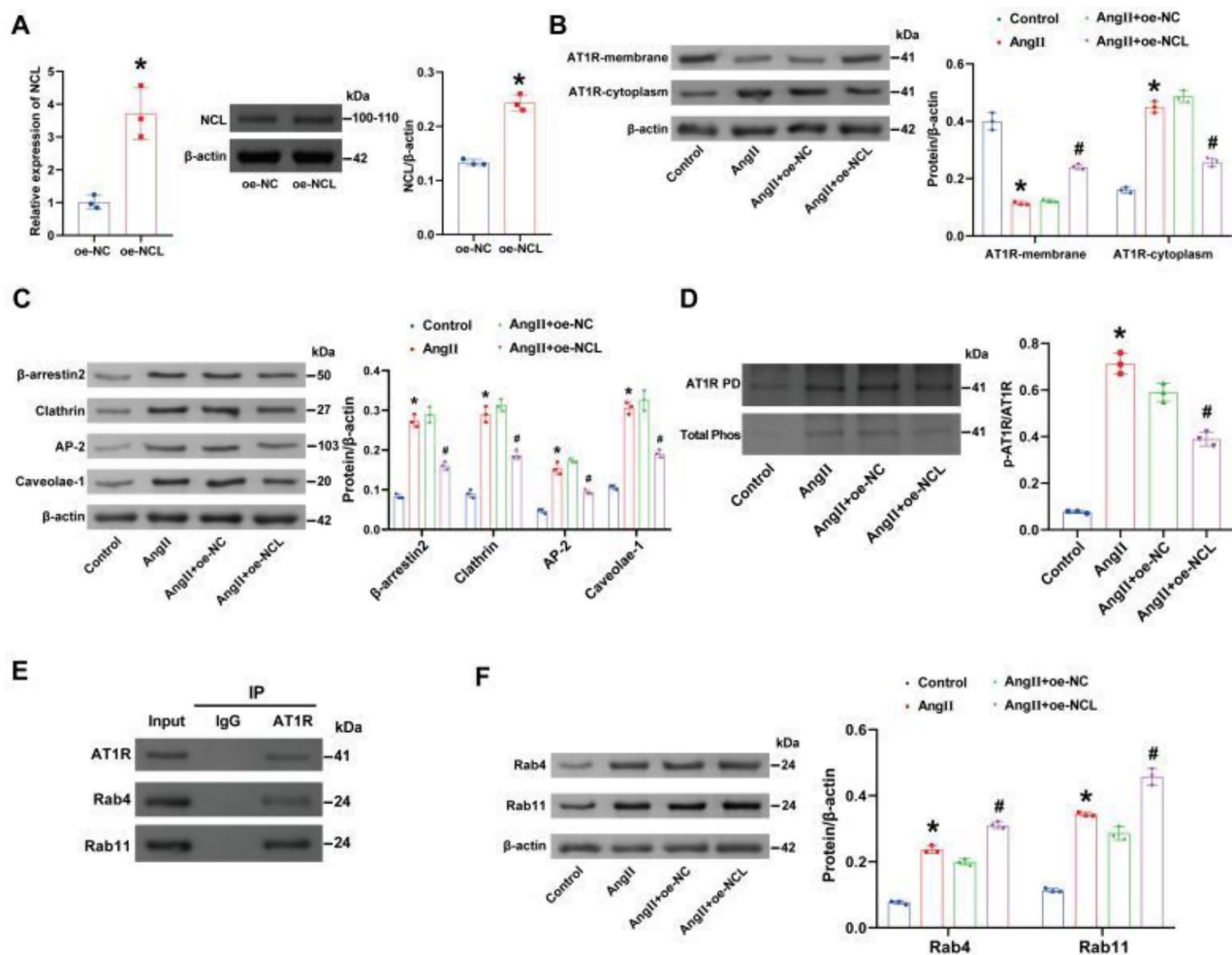


**Fig. 5** NCL delays Ang II-induced AT1R internalization and recruits Rab4 and Rab11 to promote recycling by inhibiting AT1R phosphorylation. **A.** RT-qPCR and WB analysis of NCL expression in VSMCs transfected with oe-NC or oe-NCL. \* $p < 0.05$  vs. oe-NC. **B.** WB analysis of AT1R expression in the cell membrane and cytoplasm of VSMCs. **C.** WB analysis of  $\beta$ -arrestin2, Clathrin, AP-2, and Caveolae-1 expression in VSMCs. **D.** Detection of AT1R phosphorylation in VSMCs. Pulldown Westerns are indicated by pulldown (PD). **E.** Co-IP assay for validating the binding of AT1R to Rab4 and Rab11, respectively. **F.** WB analysis of Rab4 and Rab11 expression in VSMCs. VSMCs were transfected with oe-NC or oe-NCL and then treated with Ang II. \* $p < 0.05$  vs. Control, # $p < 0.05$  vs. Ang II + oe-NC.  $n = 3$

phosphorylation, endocytosis, and recirculation). Phosphorylation is usually the trigger for AT1R. Inhibition of AT1R phosphorylation reduces the affinity of the receptor for beta-blockers thereby delaying AT1R internalization. In most cases, AT1R internalization is followed by dephosphorylation in the nuclear endosome and then recycled to the plasma membrane, leading to re-sensitization [26]. Internalization of AT1R affects not only the density of receptors at the plasma membrane but also the strength of the signaling

pathway transduction [33]. Reduced AT1R internalization may lead to aberrant AT1R activation, which promotes the development of cardiovascular diseases such as hypertension [34]. It has been shown that up-regulation of AT1R-related protein ATPAP, down-regulation of AT1R-related protein ARAP1, or increasing the ratio of ATPAP and ARAP1 decreases the internalization of AT1R, which contributes to AT1R-induced cardiovascular disease onset and progression [8]. In our study, we found that overexpression of NCL was able to delay



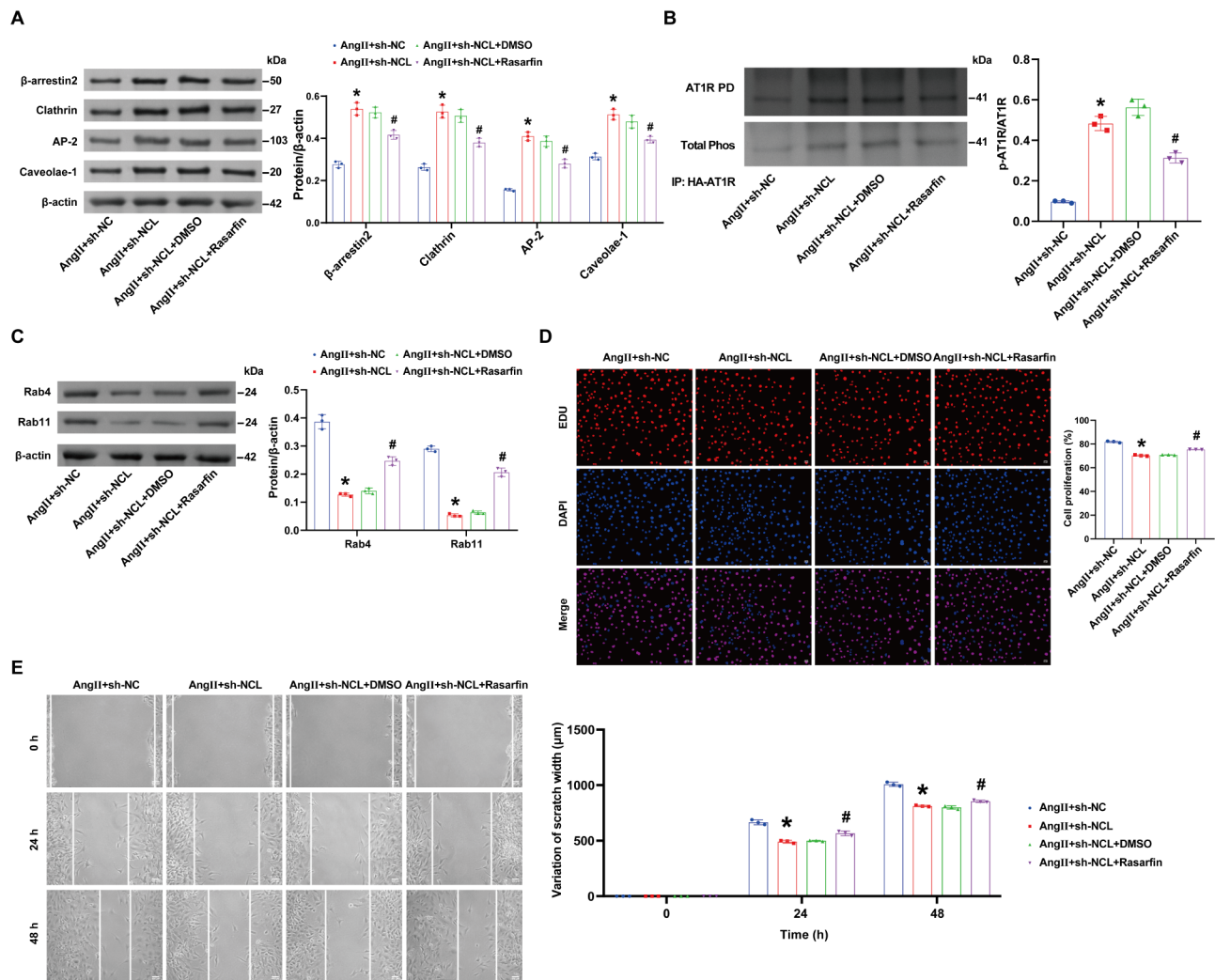


**Fig. 6** NCL induces VSMC phenotypic switching by reducing Ang II-induced AT1R internalization leading to sustained AT1R activation. VSMCs were transfected with oe-NC or oe-NCL and then treated with Ang II and 50  $\mu$ M rasafin. **A**. WB analysis of  $\beta$ -arrestin2, Clathrin, AP-2, and Caveolae-1 expression in VSMCs. **B**. Detection of AT1R phosphorylation in VSMCs. **C**. WB analysis of Rab4 and Rab11 expression in VSMCs. **D**. EDU assay for detecting cell proliferation. Scale bar = 50  $\mu$ M. **E**. Scratch assay for detecting cell migration. Scale bar = 100  $\mu$ M. **F**. WB analysis of  $\alpha$ -SMA, SM22 $\alpha$ , and OPN expression. **G**. IF assay for detecting  $\alpha$ -SMA and OPN expression. Scale bar = 25  $\mu$ M. VSMCs were transfected with sh-NC or sh-NCL and then treated with Ang II and rasafin. \* $p < 0.05$  vs. Ang II + sh-NC, # $p < 0.05$  vs. Ang II + sh-NCL + DMSO.  $n = 3$

Ang II-induced AT1R internalization by inhibiting AT1R phosphorylation. Some AT1Rs that are cytosolized into the cytoplasm can be recirculated to the plasma membrane to maintain the density of receptors at the plasma membrane, which is called recycling [35]. The current studies suggest that Rab4 and Rab11 are involved in the regulation of AT1R recycling [27, 36]. Similarly, our study confirms that Rab4 and Rab11 bind to AT1R and that overexpression of NCL promotes

the expression of Rab4 and Rab11, thereby facilitating AT1R recycling. It is the inhibition of AT1R internalization and the promotion of recycling by NCL that leads to the sustained activation of AT1R, thus inducing the VSMC phenotypic switching. In in vivo experiments, we also confirmed the above effects of NCL and demonstrated the inhibitory effect of knockdown of NCL expression on Ang II-induced blood pressure rise and vascular lesions.

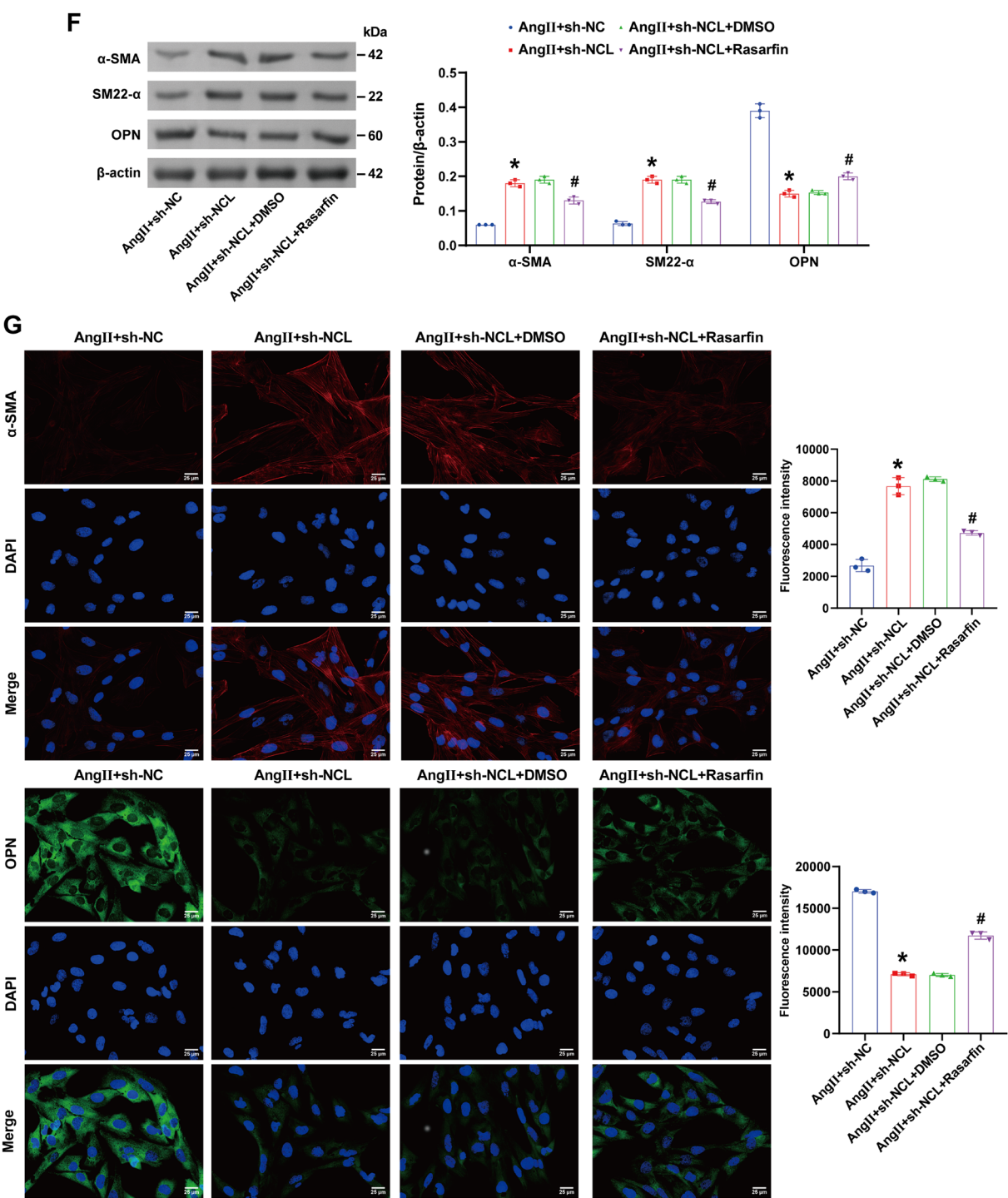


**Fig. 6** (continued)

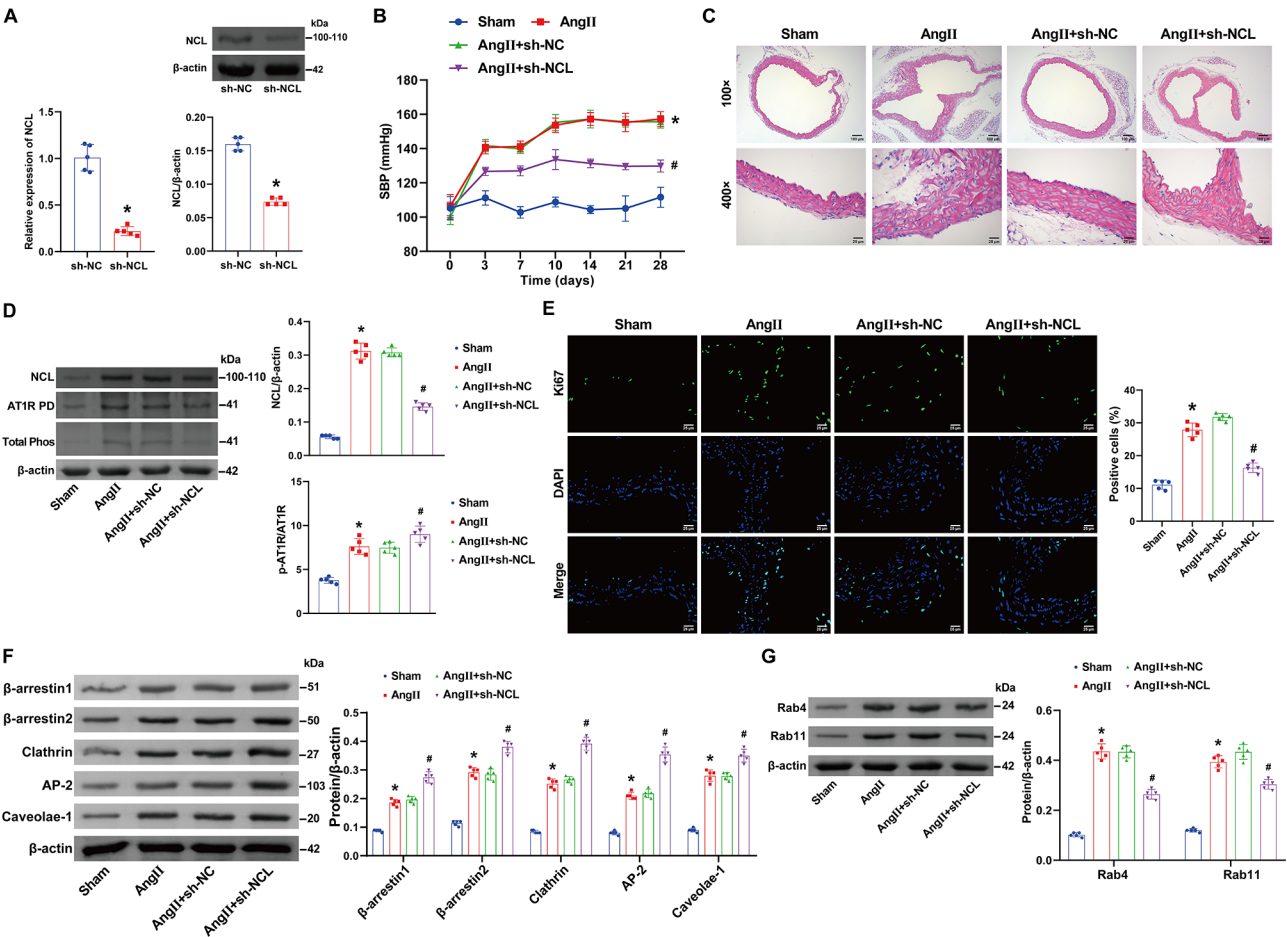


**Fig. 7** NCL promotes VSMC phenotypic switching in mice. **A**. RT-qPCR and WB analysis of NCL expression in mice. **B**. Blood pressure monitoring in mice. **C**. H&E staining of thoracic aorta from mice. Scale bar = 100 and 25  $\mu$ m. **D**. WB analysis of NCL expression. **E**. IF staining for detecting Ki67 expression. Scale bar = 25  $\mu$ m. **F**. WB analysis of  $\beta$ -arrestin1,  $\beta$ -arrestin2, Clathrin, AP-2, and Caveolae-1 expression. **G**. WB analysis of Rab4 and Rab11 expression. **H**. IF assay for detecting  $\alpha$ -SMA and OPN expression. Scale bar = 25  $\mu$ m. **I**. WB analysis of AT1R, p-p38MAPK/p38MAPK, p-JNK/JNK, p-ERK/ERK, and p-PKC $\alpha$ /PKC $\alpha$  expression. The mice were treated with Ang II and injected with sh-NC or sh-NCL lentiviruses in the tail vein. \* $p$  < 0.05 vs. sh-NC. \* $p$  < 0.05 vs. Sham, # $p$  < 0.05 vs. Ang II + sh-NC.  $n$  = 5

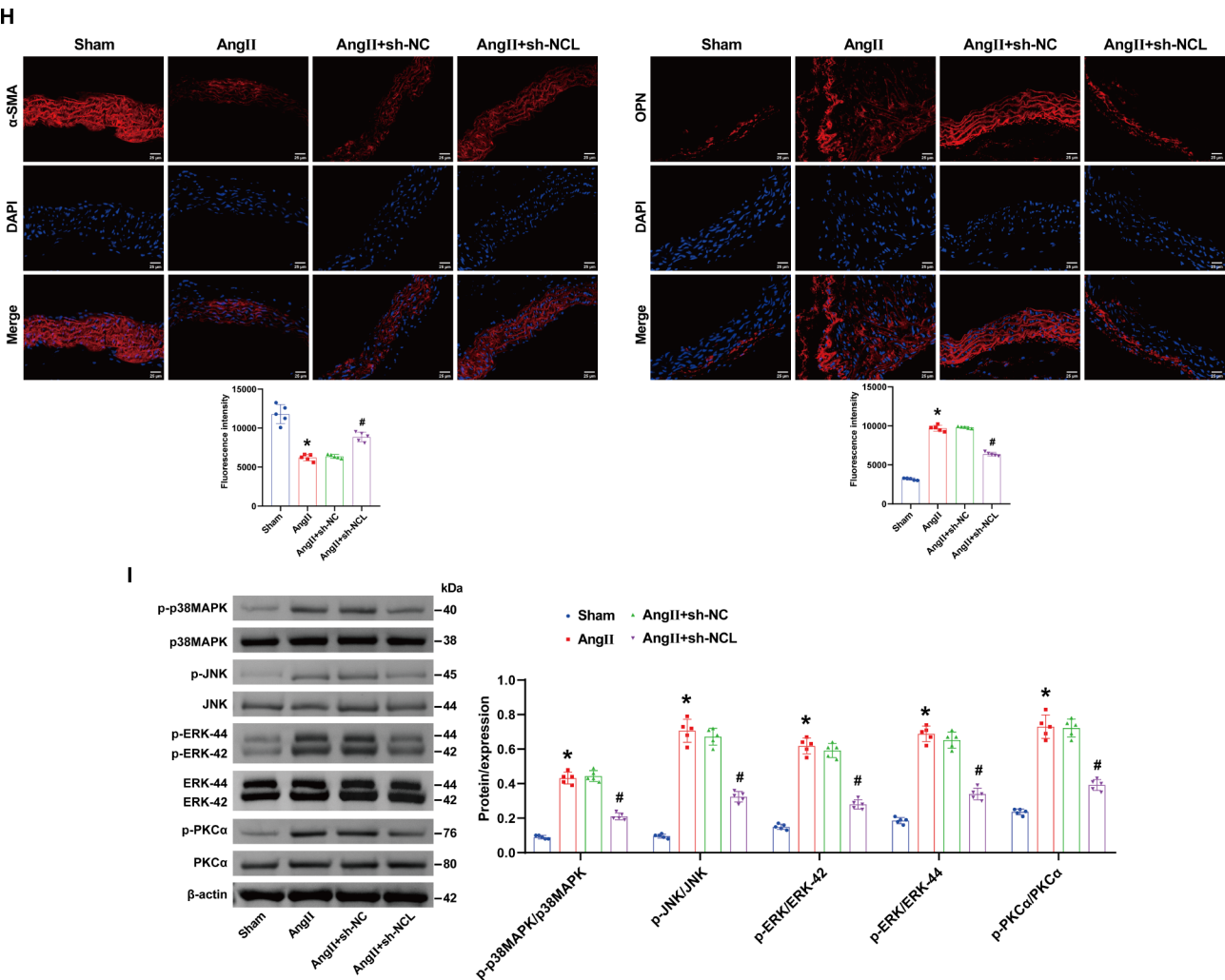


**Fig. 7** (continued)

**Conclusions**

Taken together, the present study demonstrates that NCL, a novel AT1R-associated protein, induces VSMC phenotypic switching by regulating AT1R internalization and recycling, leading to sustained activation of AT1R signaling. This provides a novel target for the treatment of cardiovascular-related diseases due to VSMC phenotypic switching.

**Supplementary Information**

The online version contains supplementary material available at <https://doi.org/10.1186/s13062-025-00615-0>.

Supplementary Material 1

**Acknowledgements**

N/A.

**Author contributions**

FL supervised the completion of this study and wrote the first draft. LF, ZS, YZ, ZM, DH and CL performed the experiments and collected the data. LF, ZS, YZ analyzed the data. ZS prepared the Figs. 1, 2, 3, 4, 5, 6 and 7. All authors read and approved the final manuscript.

**Funding**

This work was supported by grants from High-level Talent Major Scientific Research Project of the Hunan Provincial Health Commission, P. R. China (No. R2023084), Hunan Natural Science Foundation, P. R. China (No. 2022JJ30627), Changsha Natural Science Foundation, P. R. China (No. kq2202001) and Health Commission of Hunan Province, P. R. China (No. 202203012990).

**Data availability**

The datasets used and/or analysed during the current study are available from the corresponding author on reasonable request.

**Declarations**

**Ethics approval and consent to participate**

All animal experiments in this study were improved by Ethics Committee of the First Hospital of Changsha under 2022-02.



**Consent for publication**

Not applicable.

**Competing interests**

The authors declare no competing interests.

Received: 29 May 2024 / Accepted: 6 February 2025

Published online: 26 February 2025

**References**

- Cao G, Xuan X, Hu J, Zhang R, Jin H, Dong H. How vascular smooth muscle cell phenotype switching contributes to vascular disease. *Cell Commun Signal*. 2022;20(1):180.
- Grootaert MOJ, Bennett MR. Vascular smooth muscle cells in atherosclerosis: time for a re-assessment. *Cardiovasc Res*. 2021;117(11):2326–39.
- Petsophonsakul P, Furmanik M, Forsythe R, Dweck M, Schurink GW, Natour E, et al. Role of vascular smooth muscle cell phenotypic switching and calcification in aortic aneurysm formation. *Arterioscler Thromb Vasc Biol*. 2019;39(7):1351–68.
- Chakraborty R, Chatterjee P, Dave JM, Ostriker AC, Greif DM, Rzuclidlo EM, et al. Targeting smooth muscle cell phenotypic switching in vascular disease. *JVS Vasc Sci*. 2021;2:79–94.
- Sun SY, Cao YM, Huo YJ, Qiu F, Quan WJ, He CP, et al. Nicotinate-Curcumin inhibits AngII-induced vascular smooth muscle cell phenotype switching by upregulating Daxx expression. *Cell Adh Migr*. 2021;15(1):116–25.
- Dai F, Qi Y, Guan W, Meng G, Liu Z, Zhang T, et al. RhoGDI stability is regulated by SUMOylation and ubiquitination via the AT1 receptor and participates in Ang II-induced smooth muscle proliferation and vascular remodeling. *Atherosclerosis*. 2019;288:124–36.
- Alanazi WA, Alhamami HN, Alharbi M, Alhazzani K, Alanazi AS, Alsanea S, et al. Angiotensin II type 1 receptor blockade attenuates gefitinib-induced cardiac hypertrophy via adjusting angiotensin II-mediated oxidative stress and JNK/P38 MAPK pathway in a rat model. *Saudi Pharm J*. 2022;30(8):1159–69.
- Bian J, Zhang S, Yi M, Yue M, Liu H. The mechanisms behind decreased internalization of angiotensin II type 1 receptor. *Vascul Pharmacol*. 2018;103–105:1–7.
- Turu G, Balla A, Hunyady L. The role of beta-arrestin proteins in Organization of Signaling and Regulation of the AT1 angiotensin receptor. *Front Endocrinol (Lausanne)*. 2019;10:519.
- El-Arif G, Khazaal S, Farhat A, Harb J, Annweiler C, Wu Y et al. Angiotensin II type I receptor (AT1R): the Gate towards COVID-19-Associated diseases. *Molecules*. 2022;27(7).
- CA L, ML B-C. Beta-arrestins in the context of cardiovascular diseases: focusing on angiotensin II type 1 receptor (AT1R). *Cell Signal*. 2022;92:110253.
- Tonello F, Massimino ML, Peggion C. Nucleolin: a cell portal for viruses, bacteria, and toxins. *Cell Mol Life Sci*. 2022;79(5):271.
- Jia W, Yao Z, Zhao J, Guan Q, Gao L. New perspectives of physiological and pathological functions of nucleolin (NCL). *Life Sci*. 2017;186:1–10.
- Fang L, Wang KK, Zhang PF, Li T, Xiao ZL, Yang M, et al. Nucleolin promotes Ang II-induced phenotypic transformation of vascular smooth muscle cells by regulating EGF and PDGF-BB. *J Cell Mol Med*. 2020;24(2):1917–33.
- Fang L, Zhang P, Wang K, Xiao Z, Yang M, Yu Z. Nucleolin promotes Ang II-induced phenotypic transformation of vascular smooth muscle cells via interaction with tropoelastin mRNA. *Int J Mol Med*. 2019;43:1597–610.
- Samara VA, Das S, Reddy MA, Tanwar VS, Stapleton K, Leung A et al. Angiotensin II-Induced Long non-coding RNA Alivc regulates chondrogenesis in vascular smooth muscle cells. *Cells*. 2021;10(10).
- Deng Y, Li S, Chen Z, Wang W, Geng B, Cai J. Mdivi-1, a mitochondrial fission inhibitor, reduces angiotensin-II- induced hypertension by mediating VSMC phenotypic switch. *Biomed Pharmacother*. 2021;140:111689.
- Wu G, Wang Z, Shan P, Huang S, Lin S, Huang W et al. Suppression of Netrin-1 attenuates angiotensin II-induced cardiac remodeling through the PKC/MAPK signaling pathway. *Biomed Pharmacother*. 2020;130.
- Giubilaro J, Schuetz DA, Stepniewski TM, Namkung Y, Khoury E, Lara-Marquez M, et al. Discovery of a dual Ras and ARF6 inhibitor from a GPCR endocytosis screen. *Nat Commun*. 2021;12(1):4688.
- Ma H, Chen X, Mo S, Zhang Y, Mao X, Chen J, et al. Targeting N-glycosylation of 4F2hc mediated by glycosyltransferase B3GNT3 sensitizes ferroptosis of pancreatic ductal adenocarcinoma. *Cell Death Differ*. 2023;30(8):1988–2004.
- Zaccor NW, Sumner CJ, Snyder SH. The nonselective cation channel TRPV4 inhibits angiotensin II receptors. *J Biol Chem*. 2020;295(29):9986–97.
- Zhao G, Chang Z, Zhao Y, Guo Y, Lu H, Liang W et al. KLF11 protects against abdominal aortic aneurysm through inhibition of endothelial cell dysfunction. *JCI Insight*. 2021;6(5).
- Wang L, Hu C, Dong Y, Dai F, Xu Y, Dai Y, et al. Silencing IL12p35 promotes angiotensin II-Mediated abdominal aortic aneurysm through activating the STAT4 pathway. *Mediat Inflamm*. 2021;2021:1–11.
- Doron-Mandel E, Koppel I, Abraham O, Rishal I, Smith TP, Buchanan CN, et al. The glycine arginine-rich domain of the RNA-binding protein nucleolin regulates its subcellular localization. *EMBO J*. 2021;40(20):e107158.
- Losfeld ME, Khoury DE, Mariot P, Carpentier M, Krust B, Briand JP, et al. The cell surface expressed nucleolin is a glycoprotein that triggers calcium entry into mammalian cells. *Exp Cell Res*. 2009;315(2):357–69.
- Tang X, Bian J, Li Z. Posttranslational modifications in GPCR internalization. *Am J Physiol Cell Physiol*. 2022;323(1):C84–94.
- Li H, Li H-F, Felder RA, Periasamy A, Jose PA. Rab4 and Rab11 coordinately regulate the recycling of angiotensin II type I receptor as demonstrated by fluorescence resonance energy transfer microscopy. *J Biomed Opt*. 2008;13(3).
- Daniels D, Yee DK, Faulconbridge LF, Fluharty SJ. Divergent behavioral roles of angiotensin receptor intracellular signaling cascades. *Endocrinology*. 2005;146(12):5552–60.
- Doron-Mandel E, Koppel I, Abraham O, Rishal I, Smith TP, Buchanan CN et al. The glycine arginine-rich domain of the RNA-binding protein nucleolin regulates its subcellular localization. *EMBO J*. 2021;40(20).
- Losfeld ME, Leroy A, Coddeville B, Carpentier M, Mazurier J, Legrand D. N-Glycosylation influences the structure and self-association abilities of recombinant nucleolin. *Febs j*. 2011;278(14):2552–64.
- Singh KD, Karnik SS. Angiotensin receptors: structure, function, signaling and clinical applications. *J Cell Signal*. 2016;1(2).
- Wakui H. The pathophysiological role of angiotensin receptor-binding protein in hypertension and kidney diseases: Oshima Award address 2019. *Clin Exp Nephrol*. 2020;24(4):289–94.
- Tamura K, Azushima K, Kinguchi S, Wakui H, Yamaji T. ATRAP, a receptor-interacting modulator of kidney physiology, as a novel player in blood pressure and beyond. *Hypertens Res*. 2022;45(1):32–9.
- Tamura K, Wakui H, Maeda A, Dejima T, Ohsawa M, Azushima K, et al. The physiology and pathophysiology of a novel angiotensin receptor-binding protein ATRAP/Agtrap. *Curr Pharm Des*. 2013;19(17):3043–8.
- Wilson B, Flett C, Gemperle J, Lawless C, Hartshorn M, Hinde E et al. Proximity labelling identifies pro-migratory endocytic recycling cargo and machinery of the Rab4 and Rab11 families. *J Cell Sci*. 2023;136(12).
- Hu J, Zhu Z, Chen Z, Yang Q, Liang W, Ding G. Alteration in Rab11-mediated endocytic trafficking of LDL receptor contributes to angiotensin II-induced cholesterol accumulation and injury in podocytes. *Cell Prolif*. 2022;55(6):e13229.

**Publisher's note**

Springer Nature remains neutral with regard to jurisdictional claims in published maps and institutional affiliations.